



DR SIMONETTA MATTIUCCI (Orcid ID : 0000-0003-3881-095X)

Article type : Original Paper

***Anisakis pegreffii* impacts differentiation and function of human dendritic cells**

Chiara Napoletano<sup>a</sup>, Simonetta Mattiucci<sup>b§</sup>, Alessandra Colantoni<sup>b</sup> Federico Battisti<sup>a</sup>, Ilaria Grazia Zizzari<sup>a</sup>, Hassan Rahimi<sup>a</sup>, Marianna Nuti<sup>a</sup>, Aurelia Rughetti<sup>a§</sup>

<sup>a</sup>*Department of Experimental Medicine, "Sapienza" University of Rome, Italy*

<sup>b</sup>*Department of Public Health and Infectious Diseases (Laboratory affiliated to Istituto Pasteur Italia - Fondazione Cenci Bolognetti), and University Hospital "Policlinico Umberto I", "Sapienza" University of Rome, Italy*

<sup>§</sup>*Corresponding author:*

*Simonetta Mattiucci, PhD*

*Department of Public Health and Infectious Diseases, "Sapienza" University of Rome, Laboratory affiliated to Istituto Pasteur Italia-Fondazione Cenci Bolognetti e-mail: simonetta.mattiucci@uniroma1.it*

*Phone: +30 06 49914894*

This article has been accepted for publication and undergone full peer review but has not been through the copyediting, typesetting, pagination and proofreading process, which may lead to differences between this version and the Version of Record. Please cite this article as doi: 10.1111/pim.12527

This article is protected by copyright. All rights reserved.

and

Aurelia Rughetti, PhD

*Department of Experimental Medicine*

*“Sapienza” University of Rome, e-mail: aurelia.rughetti@uniroma1.it*

*Phone: +39 0649973025*

#### Abstract

Human dendritic cells (DCs) show remarkably phenotypic changes when matured in presence of helminth-derived products. These modifications frequently elicited a polarization towards Th2 cells and regulatory T cells thus contributing to immunological tolerance against these pathogens. In this study, the interaction between DCs and larvae of the zoonotic anisakid nematode *Anisakis pegreffii* was investigated. *A. pegreffii* larvae were collected from fish hosts and monocyte derived DCs were co-cultured in the presence of the live larvae (L) or its crude extracts (CE).

In both experimental conditions *A. pegreffii* impacted DC viability, hampered DC maturation by reducing the expression of molecules involved in antigen presentation and migration (i.e. HLA-DR, CD86, CD83 and CCR7), increased the phagosomal ROS levels and modulated the phosphorylation of ERK1,2 pathway.

These biological changes were accompanied by the impairment of DCs to activate a T cell mediated IFN $\gamma$ . Interestingly, live larvae appeared to differently modulate DC secretion of cytokines and chemokines as compared to CE.

Accepted Article

These results demonstrate, for the first time, the immunomodulatory role of *A. pegreffii* on DCs biology and functions. In addition, they suggest a dynamic contribution of DCs to the induction and maintenance of the inflammatory response against *A. pegreffii*.

Key words: *Anisakis pegreffii*, anisakid, dendritic cells, host-parasite interaction, inflammatory response, T cell subsets

## 1. INTRODUCTION

Anisakiasis is a zoonotic human disease provoked by the accidental ingestion of larvae of anisakid nematode belonging to the genus *Anisakis*, infecting edible parts of fish or squid, which are consumed raw and/or undercooked. These anisakid nematodes are heteroxenous parasites involving marine mammals (mainly cetaceans) as definitive hosts, while crustaceans (krill), fish and squid act as intermediate/paratenic hosts in their life cycles.<sup>1</sup> Nine species have so far been detected genetically as belonging to the genus *Anisakis*.<sup>1-3</sup> Among these, *A. simplex (sensu stricto)* and *A. pegreffii* are shown to play a zoonotic role in humans.<sup>2,4-9</sup> *A. pegreffii* infection can provoke gastric (GA), intestinal (IA) and gastro-allergic anisakiasis (GAA).<sup>2,6-11</sup>

The pathological outcomes within the gastrointestinal tract during an infection by *Anisakis* spp. larvae are the combined result of the direct invasive capacity of the larva, the antigens released during its invasion and the interaction with the host's immune response.<sup>12</sup> The larvae release proteolytic enzymes in order to invade the gastrointestinal mucosa. These antigenic proteins have been isolated and characterised as excretory/secretory antigens.<sup>13</sup> After 2-4 weeks from ingestion of the infected fish, the larva dies and its debris cause a persistent inflammation or a chronic ulceration in the gastrointestinal mucosa.<sup>14</sup> Th2 cytokines production and the resulting mastocytosis, IgE response and eosinophilia, characterise local inflammatory lesions produced by *Anisakis* spp. larvae.

Sometimes the infection can also generate mild or strong allergic symptoms such as urticaria-angio-oedema to anaphylaxis. Indeed, specific *A. pegreffii*-IgE response has been found in the serum of sensitized patients,<sup>10</sup> accompanied by a predominant Th2-type response to the parasite.<sup>13</sup> Results from murine models have confirmed that a predominant Th2 immune responses are induced by infestation with the live larvae,<sup>12</sup> while a mixed Th1/Th2 polarization is observed when the parasite crude extracts are used as immunogen.<sup>15</sup>

Generally, the immune response to helminth is triggered by damage to the epithelial cells with secretion of alarmins (TSLP, IL-33 and IL-25) and activation of antigen presenting cells such as Dendritic Cells (DCs), Innate Lymphoid Cells 2 (ILC2) and macrophages. This drives an overall activation and amplification of Th2 cell differentiation, subsequent class switching of B cells (IgA, IgE and IgG) and a promotion the migration of Th2 cells back to the site of infection.<sup>16-17</sup> Thus, the activation and the modulation of the human immune response are strictly dependent on the functions of APCs engaged by the helminth pathogens.

DCs, by sensing the tissue damage and migrating to lymph nodes, play a crucial role in the coordination of both natural and adaptive immunity and are key regulators of the adaptive immunity driving the polarization of naïve T cells towards Th subsets.<sup>18-19</sup> It has been shown that the helminth molecular repertoire impacts DC phenotype and functions.<sup>20</sup> Furthermore, several evidences suggest that helminths exert immunomodulatory effects on their hosts influencing the polarization of T cells through the modulation of DCs.<sup>21-22</sup>

The aim of this work was to investigate the mechanisms by which *A. pegreffii* influences the human immune response through the modulation of DCs. DC viability, phenotype and function were studied upon exposure to the alive larvae as well as to their crude extracts (CE). The immunomodulatory effects exerted by *A. pegreffii* on DCs could be a biological mechanism contributing to host immune evasion by the parasite and could contribute to the chronic inflammatory response evoked by this zoonotic parasite.

## 2. MATERIALS AND METHODS

### 2.1 Parasites

Live *Anisakis* sp. larvae were removed from the viscera and body cavity of the fish host (anchovy, *Engraulis encrasicolus* and European hake, *Merluccius merluccius*) caught from the Adriatic Sea (off S. Benedetto del Tronto coast). After their removal from the fish host, they were first washed in 4% acetic acid (Carlo Erba, Cornaredo, Italy) and then in phosphate-buffered saline (PBS, Sigma, St Louis, MO). A batch of these larvae was then transferred to the *in vitro* culture (see below), whereas another one was used for the CE preparation. The larvae used for *in vitro* culture, after their removal from the culture, were stored at -20°C, for their identification to the species level.

### 2.2. Molecular identification of *Anisakis* sp. Larvae

A subsample ( $N= 50$ ) of those *Anisakis* spp. larvae used for *in vitro* culture and by CE preparation, was identified to the species level by means of genetic/molecular markers. For this purpose, a multi-locus approach based sequences analysis of mitochondrial (mtDNA *cox2*) (629 bp) and nuclear (elongation factor EF1  $\alpha$ -1 of nDNA) (409 bp) genes was performed.<sup>3,23</sup> The genomic DNA was extracted using the Quick-gDNA MiniPrep (column format) by Zymo Research from 2 mg of homogenized tissue from each single nematode following the manufacturer's protocol.

The mitochondrial cytochrome c oxidase subunit II (*cox2*) gene was amplified using the primers 211F (5'-TTTTCTAGTTATATAGATTGRTTYAT-3') and 210R (5'-CACCAACTCTTAAAATTA TC-3'). Polymerase chain reaction (PCR) was carried out according to the procedures as previously described.<sup>3</sup> The sequences obtained at the mtDNA *cox2* for those larval specimens analyzed in the present study were compared with those already obtained for the same gene in the species *A. pegreffii* and with respect to those from other *Anisakis* spp. previously sequenced.<sup>2-3</sup>

The elongation factor (EF1  $\alpha$ -1 nDNA) nuclear gene was amplified using the primers EF-F (5'-TCCTCAAGCGTTGTTATCTGTT-3') and EF-R (5'-AGTTTTGCCACTAGCGGTTCC-3') and employing experimental conditions, as previously described.<sup>23</sup> The sequences obtained at the EF1  $\alpha$ -1 nDNA for the larval specimens analyzed in the present study were compared with those already obtained for the same gene in the species *A. pegreffii* and *A. simplex* (s. s.), under the accession numbers KT825684 and KT825685, respectively.

The genomic DNA obtained from those samples are stored at the research laboratory of S. Mattiucci, Department of Public Health and Infectious Diseases (Section of Parasitology) - 'Sapienza University of Rome'.

### 2.3 Preparation of *A. pegreffii* L3 Crude Extracts (CE)

Crude Extracts (CE) of *A. pegreffii* larvae were prepared as follows: each larval part was rinsed in physiological saline, then homogenised with PBS 10X and proteinase inhibitors in a mortar; the homogenate was then centrifuged at 14,000 rpm for 30 min at 4°C; finally, the supernatant was retained. Protein concentration from CE was determined using the Quick Start Bradford Protein Assay (Bio Rad, Berkeley, CA) with Bovine Serum Albumin as a standard control.

### 2.4 DC generation

DCs were produced as previously described.<sup>24</sup> Briefly, peripheral blood mononuclear cells (PBMCs) were isolated by Ficoll-Hypaque gradient (1,077 g/mL; Pharmacia LKB, Upsala, Sweden) from buffy coats of healthy donors obtained by the Transfusion Center, Policlinico Umberto I – "Sapienza" University of Rome (Ethics Committee - Protocol nr. 4212). Monocytes (Mo, CD14<sup>+</sup>) were purified from PBMCs by CD14 MicroBeads (Miltenyi Biotech, Paris, France) and cultured in RPMI 1640

(Hyclone, South Logan, Utah) with 10% heat-inactivated FCS (Hyclone). GM-CSF (50 ng/mL; R&D Systems, Oxon, UK) and 2,000 units/mL of rhIL-4 (R&D System) were added at day 0 and 2 for differentiation in immature DCs (iDCs). On day 5, iDCs were collected and matured for 24 hours with cytokine cocktail (rhIL-1 $\beta$ , rhIL6, TNF $\alpha$  (10 ng/mL each; R&D) and PGE<sub>2</sub> (1mg/mL; R&D). On day 6, iDCs were considered mature (mDCs). For all the experiments, the CE of *A. pegreffii* (40  $\mu$ g/mL/10<sup>6</sup> cells) were added to the Mo at day 0 and day 2 of differentiation, for a total of 80  $\mu$ g/mL throughout the culture, while the live larvae L3 were added to the cells at day 0 until the end of the culture (7 larvae/6x10<sup>5</sup> cells/mL). In parallel, live larvae L3 were seeded in culture medium in absence of DCs (7 larvae/mL) following the same DC culture procedure (addition of IL4 and GM-CSF cytokines at day 0 and 2 and addition of maturative stimuli at the end of the culture). The number of larvae added to the culture was chosen to assure the presence in the culture of 80  $\mu$ g of secreted proteins [average yield of secreted proteins/larva of 20  $\mu$ g; viability of the larva (evaluated as motility) at the end of culture resulted  $\geq$  4/7].

## 2.5 DC phenotype

Cell phenotype staining was performed using the following panel of mouse monoclonal antibodies (MoAbs) directly conjugated with fluorescein isothiocyanate (FITC) or phycoerythrin (PE): IgG<sub>1</sub> or IgG<sub>2b</sub> FITC and IgG<sub>1</sub> or IgG<sub>2b</sub> PE, as isotype controls, anti-HLA-DR FITC, anti-CD86 FITC, anti-CCR7 FITC, anti-CD83 PE, anti-CD14 PE, and anti-CD40 PE all purchased from eBioscience (San Diego, CA, USA). On day 6, iDCs and mDCs were suspended in PBS without Ca<sup>2+</sup> and Mg<sup>2+</sup> (Hyclone) (2x10<sup>5</sup> cells/100 mL/sample) and incubated with the monoclonal antibodies according to manufacturer's instructions. At least 1x10<sup>4</sup> events were evaluated using a FACSCanto flow cytometer (Becton Dickinson, San Diego, CA) running FACSDiva acquisition and analysis software (Becton Dickinson).

## 2.6 DC Apoptosis

Apoptosis of DCs was evaluated using the FITC Annexin V Apoptosis Detection Kit I (Becton Dickinson) according to the manufacturer's instructions. Briefly,  $10^5$  DCs were resuspended in 100 $\mu$ l of Binding Buffer 1X with 5 $\mu$ L of FITC Annexin V and 5 $\mu$ L Propidium Iodide (PI) for 15 minutes at Room Temperature (RT). After incubation, 400 $\mu$ L of Binding Buffer were added to the cells that were then analysed using a FACSCanto flow cytometer (Becton Dickinson) running FACSDiva acquisition and analysis software (Becton Dickinson). Data were reported as percentage of live cells.

## 2.7 Immunoblotting (WB)

On day 6, differently treated DCs ( $10^6$  cells/sample) were centrifuged, resuspended in 50-100  $\mu$ L of PBS without  $\text{Ca}^{2+}$  and  $\text{Mg}^{2+}$  (Hyclone) and lysed by freeze and thaw. Cellular lysates were subjected to 10% SDS-PAGE and the resolved proteins were transferred electrophoretically to nitrocellulose transfer membrane (Whatman, Dassel, Germany). After blocking with PBS + 5% BSA for 16 to 18 h at 4°C, membranes were incubated with the mouse MoAb anti-pERK1,2 (1:1,000; Cell Signaling Technologies, Boston, MA, USA), anti-p50/105 (1:1,000, Cell Signaling Technologies) and anti- $\alpha$ -Tubulin (1:1,000; Santa Cruz Biotechnology, Dallas Texas, USA) for 16-18 hours, overnight. Membranes were then treated with peroxidase-conjugated goat anti-mouse IgG (1:20,000, H+L; Jackson ImmunoResearch Laboratories, Pennsylvania, USA) for 1 h at room temperature. The protein bands were detected with enhanced chemiluminescence reagents (Merck Millipore, Darmstadt, Germany) following the manufacturer's instructions.



## 2.8 DC Phagosomal ROS measurement

Phagosomal ROS of DCs were measured as previously described.<sup>25</sup> Briefly, DCs were pulsed with 3  $\mu\text{m}$  microbeads (Polysciences Inc) coupled with Dihydrorhodamine 123 (DHR123; ROS sensitive, Life Technologies, Carlsbad, CA, USA) and FluoProbes 647 (ROS insensitive, Interchim, Montlucon, San Diego, USA) for 15 minutes at 37°C. After extensively washing with cold PBS, DCs were incubated at 37°C for 15 minutes and analysed by FACS (FACSCanto, Becton Dickinson), using a FL1 (DHR123)/FL4 (FluoProbes 647) gate selective for cells that had phagocytosed 1 latex bead.

The ratio between Mean Fluorescence Intensity of DHR123 (FL1) and FP647 (FL4) of iDCs control group was set as 100% of relative ROS production. The ROS measurement for the other DC samples were obtained by comparing the ratio of DHR123/FP647 for each DCs sample with the ratio of control DCs expressed AS 100%. Supplementary Figure 1 depicts the gating strategy, normalization of the MFI and the results of a representative donor.

## 2.9 Intracellular cytokine staining of autologous CD4<sup>+</sup> T cells

On day 6, differently treated DCs were collected and plated in  $75 \times 10^4$  cells/sample in 200  $\mu\text{L}$  of complete RPMI 1640 medium in 96 well plates (Corning Incorporated, New York, USA). Autologous CD4<sup>+</sup>CD45RA<sup>+</sup> purified T cells (Miltenyi) were added to DC cultures at 1:2 ratio. After 4 days of co-culture, cells were stimulated with PMA (25 ng/mL) (Sigma) and Ionomycin (250 ng/mL) (Sigma) and were incubated with Brefeldin A (10 mg/mL, Sigma) for 16 to 18 hours at 37°C and 5%CO<sub>2</sub>. T cells were collected, fixed, and permeabilized with Saponin (Sigma) solution at 0,5%. Intracellular staining was performed using the following MoAbs: FITC-conjugate anti-IFN $\gamma$  (Biolegend, San Diego, CA), APC-conjugate anti-IL17A (eBioscience), PE-conjugate IL10 (BD pharmingen, San Diego, CA) and PerCP/Cy5.5-conjugate anti-IL4 (Biolegend). Stained cells were analysed by FACSCanto flow cytometer (Becton Dickinson) running FACSDiva data acquisition and analysis software (Becton

Dickinson). Supplementary Figure 2 depicts the gating strategy and the analysis of the IFN $\gamma$  T cell response for each experimental condition of a representative donor.

#### 2.10 DC cytokine and chemokine measurements

At the end of the culture, DCs were harvested and plated  $10^6$  cells/mL in 48 well plates (Corning Incorporated). PMA (25 ng/mL) (Sigma) and Ionomycin (250 ng/mL) (Sigma) were added to the cells for 48 hours at 37°C and 5%CO $_2$ . Culture supernatants were then collected and analysed using the ProcartaPlex Human Inflammation Panel (20 Plex) (eBioscience). Samples were measured by BioPlex Magpix Multiplex Reader (Bio-Rad, Hercules, CA, USA) and data analysis was performed using Bioplex Manager MP software (Bio-Rad). Raw data were then analysed and plotted in percentage as previously shown.<sup>21</sup> PMA/Ionomycin treated iDCs or mDCs were considered as control samples and the obtained values were set as 100%. The value of the secreted cytokine of each experimental DC group (DCs+CE, DCs+L) was compared to the corresponding DC control group. Such procedure was adopted to analyse three independent experiments conducted employing DC cultures obtained from three healthy donors. The average and the standard deviation of the percentage value obtained for each DC experimental group among the three cultures was calculated and plotted as histogram.

#### 2.11 Statistical Analysis

Descriptive statistics (average and standard deviation) were used to describe various groups of data. ANOVA test was used to analyze statistical differences between three groups. Student's paired *t*-test was used to compare two groups. Significance level was  $p \leq 0.05$ .

### 3. RESULTS

#### 3.1 Molecular identification of *Anisakis* spp. larvae

The subsample ( $N=50$ ) of *Anisakis* L3 larvae used in the present study, was assigned to the species *A. pegreffii* on the basis of the sequences analysis of the mitochondrial and nuclear gene loci studied. mtDNA *cox2* sequences obtained from the larval nematodes used for the antigen preparations showed 99% or 100% similarity with sequences previously deposited in GenBank for *A. pegreffii*.<sup>3</sup> In addition, phylogenetic analysis inferred from MP (Figure 1), showed that the sequences obtained at the mtDNA *cox2* gene from those *Anisakis* spp. larvae clustered in a well supported clade also including the sequence of *A. pegreffii* for that gene, previously obtained and deposited in GenBank. The clade represented by *A. pegreffii* was also distinct from the other phylogenetic lineages represented by the other *Anisakis* spp. (Figure 1). Some sequences of mtDNA *cox2* among those obtained were deposited in GenBank under the accession numbers: KY418057-KY418062.

Finally, according to the diagnostic positions found at the 409 bp in length of the EF1  $\alpha$ -1 nDNA region - i.e. 186, showing a T in *A. pegreffii*, and the position 286, showing a C in *A. pegreffii*<sup>23</sup> larval specimens were assigned to the species *A. pegreffii* (Figure 2). Some sequences of EF1  $\alpha$ -1 nDNA were deposited in GenBank under the accession numbers: KY703438 - KY703443.

#### 3.2 Live larvae of *A. pegreffii* affect DC survival and phenotype and modulate Erk1,2 pathway

During infection, *A. pegreffii* larvae penetrate the mucosa and migrate into the tissue. To evaluate whether during this stage the molecular repertoire released by the larvae can affect differentiation and function of DCs, CD14<sup>+</sup> monocytes from healthy donors (4) were co-cultured with parasite larvae (7 larvae/well) and differentiated in DCs (iDCs+L). The larvae were maintained in culture also after the addition of maturing *stimuli* to DCs (mDC+L).

The cell viability was initially evaluated detecting the incorporation of Propidium Iodide and the positivity to the staining with Annexin V (Figure 3A). Results were plotted as percentage of live cells, using iDCs and mDCs as controls (results of a representative donor among the four analysed are reported in Supplementary Figure 3B). The larvae of *A. pegreffii* induced the apoptosis of a high amount of DCs compared to controls, significantly reducing the percentage of live DCs both before and after maturation (iDCs vs iDC+L,  $92\% \pm 8\%$  vs  $40\% \pm 25\%$ ,  $p < 0.01$ ; mDCs vs mDC+L,  $95\% \pm 2\%$  vs  $55\% \pm 12\%$ ,  $p < 0.01$ ). At the end of the culture, *A. pegreffii* larvae in co-culture with DCs showed still motility ( $\geq 4/7$ ), similarly to the larvae seeded in the well in absence of DCs (data not shown).

The phenotype of iDCs+L and mDCs+L was then analyzed by monitoring the expression of HLA-DR, CD86 and CD40 costimulatory molecules, the differentiation marker CD83, the chemokine receptor CCR7 and the monocyte marker CD14. (A representative analysis is shown in Supplementary Figure 3B). iDCs+L expressed significantly lower levels of HLA-DR and higher levels of CD86 and CCR7 compared to iDCs. After maturation, mDC+L displayed a significant down-regulation of the HLA-DR and CCR7 compared to mDCs (Figure 3B). CD83 marker was strongly down-regulated in mDCs+L compared to control DCs, albeit this decrease was not statistically significant (MFI of mDCs vs mDCs+L, 448 vs 188,  $p = 0.06$ ). CD14 was negative in all samples and no differences in the CD40 expression was observed (data not shown).

DCs were also analyzed for the intracellular signalling triggered by the exposure to the live parasite. In particular, the activation of NF- $\kappa$ B (p50) and ERK1,2 pathways were evaluated by western blotting (Figure 3C). Results demonstrated that in immature DCs, activation of the NF- $\kappa$ B pathway and phosphorylation of ERK1, 2 kinase were similar in the absence or in the presence of the live parasite. After DC maturation, a strong decrease of the ERK1,2 signal was observed in mDCs+L compared to control, while the activation of NF- $\kappa$ B pathway remained unaltered.

### 3.3 CE of *A. pegreffii* induces apoptosis of DCs and modulates DC phenotype

To determine whether CE derived from L3s of *A. pegreffii* *per se* could affect the survival and the phenotype of DCs, the cells were also differentiated and matured in presence of the CE (iDCs+CE and mDCs+CE, respectively) and analysed by flow cytometry as shown for a representative donor among nine in Supplementary Figure 2.

As described for the larvae, the presence of the CE in the culture medium significantly decreased the percentage of live cells compared to controls (iDCs vs iDC+CE,  $90\% \pm 10\%$  vs  $60\% \pm 10\%$ ,  $p < 0.05$ ; mDCs vs mDC+CE,  $85\% \pm 10\%$  vs  $63\% \pm 8\%$ ,  $p < 0.05$ ) (Figure 4A). In addition, the CE strongly affected DC phenotype (Figure 4B). iDC+CE expressed lower levels of HLA-DR and CD86 compared to iDCs, while no difference was observed in the other DC markers. After maturation, HLA-DR, CD86, CD83 and CCR7 molecules remained lower than mDCs, while CD14 and CD40 molecules were not modified (data not shown).

The analysis of NF $\kappa$ B and ERK1,2 pathways showed that the exposure of iDCs to *A. pegreffii* CE induced a slight increase of both signalling pathways as compared to control iDCs. Conversely, the maturation process strongly reduced the phosphorylation of ERK1,2 in mDCs+CE, while the NF $\kappa$ B signalling was similar in both mDCs+CE and mDCs (Figure 4C).

### 3.4 Phagosomal ROS level in DCs are increased following exposure to *A. pegreffii*

We then investigated whether the antigen presenting machinery of DCs was altered by DCs-*A. pegreffii* interaction by evaluating the phagosomal Radical Oxygen Species (ROS) levels in DCs. The radical cargo in the phagosomal compartment is crucial to regulate antigen cross-presentation, a unique ability of DCs that allows antigen cross-priming.<sup>26</sup>

Phagosomal ROS levels were measured by flow cytometry in DCs exposed to both live larvae and CE, before and after DC maturation (Figure 5). ROS production in both iDCs and mDCs appeared to be significantly modulated by the exposure to CE or live larvae ( $p < 0.001$ ). In the presence of *A. pegreffii*, both the live larvae and CE, the phagosomal ROS of iDCs were significantly increased compared to control iDCs ( $p < 0.001$ ).

Following maturation, again phagosomal ROS levels were strongly upregulated in the presence of both parasite larvae and crude extracts formulations than control DCs ( $p < 0.001$ ). These results show that the exposure to parasite modulates phagosomal ROS accumulation in DCs, making these cells more similar to macrophages.

### 3.5 Chemokine/Cytokine pattern released by DCs is differently modulated by *A. pegreffii* live larvae and CE

DCs release different type of cytokines and chemokines according to the type of the *stimulus* in the microenvironment.<sup>27</sup> At the end of the culture, differently treated DCs were stimulated with PMA and Ionomycin for 48 hours and the supernatants were analysed for the presence of inflammatory mediators. DC cultures from three distinct healthy donors were analysed. The results were plotted setting the values of the control DC samples (iDCs and mDCs) as 100% (Figure 6). In the presence of the live larva (DCs+L), DC production of CXCL10, CCL4 chemokines and sICAM were significantly downregulated, independently of the maturation stage. The exposure of DCs to CE induced a mild and not significant reduction of the CXCL10, CCL4 and sICAM. Interestingly, CCL3 chemokine was strongly upregulated in both DCs+L (immature and mature,  $p < 0.001$  and  $p < 0.05$ , respectively) and significantly increased in mDCs+CE ( $p < 0.01$ ).

The pro-inflammatory cytokines IL6, and in particular IL1 $\alpha$  were strongly up-regulated. IL6 increased significantly in immature DCs exposed to both live larvae and CE ( $p < 0.01$ ); in mDCs the IL6 response was still high, but more heterogeneous among donors. IL1 $\alpha$  secretion was enhanced particularly by the exposure of DCs to the live larva (iDCs+L:  $p < 0.05$ ; mDCs+L:  $p < 0.001$ ), while the presence of CE induced a slight although significant IL1 $\alpha$  secretion in iDC ( $p < 0.05$ ).

*A. pegreffii* impacted DCs for the production of T cell polarizing cytokines. The immunosuppressive cytokine IL10 was consistently reduced in the presence of live larva (iDCs+L and mDCs+L:  $p < 0.001$ ).

Following exposure of DCs to CE, a trend in IL10 reduction was observed in iDCs+CE, while a slight but not significant increase was detected in mDCs+CE.

IL4 production was modulated contrariwise in iDCs exposed to the live larva or to CE. In fact, IL4 dampened in iDC+L ( $p < 0.05$ ), while it increased in iDCs+CE. A similar trend was observed in mDCs.

Interestingly, the two *A. pegreffii* preparations differently affected GM-CSF secretion. DCs exposed to live larva were poor producer of GM-CSF ( $p < 0.001$ ); whereas, a trend of increase was observed in mDCs exposed to CE.

3.6 DCs exposed to *A. pegreffii* are poor inducer of Th1 response.

The ability of differently treated DCs to polarize naïve T cells towards Th1, Th2 and Th17 phenotype was studied. On day 6, iDC $\pm$ L or CE and mDCs $\pm$ L or CE were collected and incubated with autologous CD4<sup>+</sup>CD45RA<sup>+</sup> T cells for 4 days. T cells were then stimulated with PMA and Ionomycin for 16-18h and the production of IFN $\gamma$ , IL4, IL10 and IL17 was evaluated as intracellular cytokine staining (Figure 7). The presence of both the live parasite and the CE during DC differentiation exclusively hampered the production of IFN $\gamma$  by T cells, while IL4, IL17 and IL10 production were not affected.

In particular, IFN $\gamma$  mediated T cell response was significantly reduced in response to iDCs+CE with respect to control mDCs ( $p < 0.05$ ); while, a trend in IFN $\gamma$  cytokine decrease was observed upon

stimulation of iDC+L and both mDC+L/CE.

#### 4. DISCUSSION

In this study, we investigated for the first time the immunomodulatory effects of *A. pegreffi* on the differentiation and function of DCs, showing that DCs contribute to the inflammatory chronic response to the parasite by sustaining a strong inflammatory microenvironment and modulating their ability to recruit immune cells at the infection site.

DCs are antigen presenting cells equipped with a complex array of dynamically regulated receptors that endow them to sense the microenvironment and to interact with the other cells of the immune system, thus modulating their functions in response to pathogen interactions.<sup>28</sup>

In *Anisakis* infections, the tissue resident APCs first encounter the parasite, while the larva actively penetrates the gastrointestinal mucosa and migrates into the tissues.

In the following weeks, APCs are exposed to the necrotic debris released by the dying larvae and to the stress signals of the damaged tissues.

As *in vitro* model, monocyte derived differentiating DCs were exposed to L3 stage live larva or its crude extracts.

The use of the live larvae allows the direct interaction of differentiating DCs with the molecular determinants of the cuticle layer and the whole molecular repertoire actively released by the larvae, similarly to what happens *in vivo*.

This *in vitro* system also prevents the possible loss of parasite released components as such as microvesicles,<sup>29</sup> due to the purification of the secretory product. The release of necrotic debris of the dead parasite after infection was mimicked by the CE obtained from the same larvae.



The first striking effect observed was the decrease of DC viability due to the induction of apoptosis in the presence of the live larvae as well as CE. Apoptosis is adopted by helminths to dampen host immune responses<sup>30-31</sup> and to invade tissues.<sup>32-33</sup> Recently, apoptosis of fibroblast exposed to *A. pegreffii* was observed.<sup>34</sup> Here, we report that apoptosis is employed by *A. pegreffii* as a mechanism of immune escape, strongly reducing DC viability throughout the infection phases.

*A. pegreffii* also appeared to strongly impact DC differentiation and maturation. The presence of both the alive larvae as well as the CE in culture generated DCs with an impaired phenotype as demonstrated by the lack of CD83 expression, marker of DC differentiation lineage, low expression of HLAII-DR $\gamma$  and CD86 costimulatory molecules that are required for the activation of a strong immune response. The chemokine receptor CCR7, crucial for DC homing to lymph nodes, was downregulated suggesting that DCs are immobilized in the tissue, thus undermining T and B cell priming in the lymph nodes.<sup>35</sup>

The impairment of DC maturation is a common immunosuppressive mechanism adopted by many helminths.<sup>36</sup> Exposure to excretory/secretory products of *Trichinella spiralis* induces immature features in both mouse and human DCs activating a Th2 polarization and/or regulatory T cell responses.<sup>37-38</sup> Soluble products from *Schistosoma mansoni* induce up-regulation of OX40L and modulation of pro-inflammatory cytokines produced by DCs contributing to Th2 skewing.<sup>36</sup> Also, DC phenotype and maturation are impaired upon exposure to nematodes as *Trichuris suis* or *Ascaris lumbricoides*, *A. suum*, Th2 responses.<sup>21,39-40</sup>

Other important biological features of DCs affected by *A. pegreffii* were the intracellular signalling, the phagosomal activity and the secretion of pro-inflammatory and regulatory cytokines.

The interactions with pathogens induce the reprogramming of DC signalling: in particular, the balance between ERK1,2 and NF $\kappa$ B pathways seems to be a critical parameter for DC activation.<sup>41</sup>

The presence throughout DC differentiation of *A. pegreffii* (both live larvae and CE) strongly

decreased ERK1,2 pathway after DC maturation, while NF $\kappa$ B signal was not affected. These results appear in contrast with previous evidences showing a transient activation of ERK1,2 pathway in DCs following a short-time exposure to helminth components.<sup>42-43</sup> The type and the duration of the pathogenic stimulus seem to differently modulate phosphorylation of this kinase and to drive distinct cellular behaviours.<sup>41</sup> Furthermore, other DC signalling pathways could be involved and further studies are required to precisely trace the triggering induced by *Anisakis* infestation.

*A. pegreffii*, both as live larvae or as CE, led to a strong increase of Radical Oxygen Species (ROS) in the phagosomal compartment. This is a feature of macrophages and not DCs.<sup>26</sup> Recently, increased cellular ROS levels have been described as a response of fibroblasts to *A. pegreffii*.<sup>34</sup> In DCs, phagosomal ROS levels modulate antigen degradation and therefore impact HLAII/HLAI presentation and activation of CD4/CD8 T cells.<sup>26</sup> This suggests that DCs exposed to *A. pegreffii* have antigen presenting machinery favouring CD4<sup>+</sup> mediated T cell responses.

Interestingly, cytokine production by DCs was differently modulated by the live larva compared to the CE. Indeed, IL4, cytokine required for Th2 polarization, was modulated contrariwise in iDCs exposed to the live larvae or to CE: IL4 dampened in iDCs+L (p<0.05), while it increased in iDCs+CE (p<0.01). Also IL10 secretion by DCs was reduced in the presence of the live larva, while the CE did not exert any significant effect on IL10 production.

Furthermore, the pro-inflammatory cytokines IL1 $\alpha$  and, remarkably, IL6 were significantly enhanced by both formulations of *A. pegreffii*, although the live larva exerted the stronger effect.

These results suggest that while DCs may contribute to establish local inflammation since the early stages of infection, they do not clearly contribute to cytokine environment for Th2 polarization.

Indeed, autologous CD4<sup>+</sup> T cells, stimulated by DCs differentiated in the presence of live larvae or CE, failed to produce IL4, IL17 and IL10 suggesting that DCs were not sufficient to drive Th2/Th17 or Treg polarization.<sup>44</sup> However, T cells displayed a remarkable decrease of IFN $\gamma$  production, particularly

significant in iDCs, suggesting that DC driven Th1 polarization was impaired.

The Th2 response against helminths is regulated by a complex cell network: alternative activated macrophages, ILC2, fibroblasts, mast cells, damaged epithelial cells release cytokines with overlapping regulatory functions.<sup>45</sup> IL4 and IL13, the cytokines required for the Th2 skewing and granuloma formation are produced by basophils, ILC2 and IL13 is amplified by Th2 cells. Recently, Tuft cells, a rare epithelial cell type of the steady state intestinal epithelium, able to amplify in response to IL4, have been shown to be responsible for initiation of the type 2 response to helminth parasites.<sup>46</sup>

In our system, DCs exposed to the live larvae acquired features of impaired ability to recruit immune cells: the downregulation of CXCL10 and CCL4, chemokines involved in the migration of leukocytes,<sup>47</sup> counteracted the signals for recruitment given by the increase in CCL3 production and by sICAM downregulation.<sup>48-49</sup> Furthermore, DCs dampened the production of GM-CSF, a mediator of the cross-talk between myeloid cells and T cells in the inflamed tissues.<sup>50</sup>

When DCs were exposed to CE, as it happens when the larva is dying *in vivo*, CCL3 increased and CXCL4, CCL4 and GM-CSF levels were similar to control DCs, suggesting a possible role of DCs in the recruitment of immune cells.

Taken together, these results suggest that DCs might participate to the complex scenario of the immune reaction to *A. pegreffii* infection, according to the infection phase. At the first step, the live larva induces apoptosis, DCs differentiation and maturation and reduces DC ability to migrate to the lymph node. Such DCs contribute to generate an inflammatory microenvironment (IL1 $\alpha$  and IL6 increase) to sustain the plasticity for Th differentiation, while blocking Th1 polarization (reduced IFN $\gamma$  T cell responses) and altering leukocytes recruitment. When the parasite undergoes cell death, the necrotic debris still induces apoptosis and prevents DCs to migrate to the lymph node. The tissue resident DCs upregulates CCL3 chemokine that may favour leukocyte recruitment during granuloma

formation and production of IL4, that in combination with IL6 might contribute to redirect T cells towards Th2 differentiation.<sup>51</sup>

Which are the ligands in *A. pegreffii* that are involved in such immunomodulatory effects remains an open question. Recently, the C-type lectin receptors, recognizing carbohydrate ligands, seem to play a key role in triggering immunosuppressive functions of DCs by helminths.<sup>21, 52-53</sup> Interestingly, *Ani s* 7, among the major allergens in *A. pegreffii*,<sup>10</sup> is indeed a glycoprotein.<sup>54</sup>

The post-translational modification that decor the protein array of the anisakid species *A. pegreffii* may be extremely relevant to understand the mechanisms underlying the impact of the parasite on innate immunity and DCs, in particular in order to manage and prevent the immune-mediated pathological responses caused by this zoonotic parasite.

#### ACKNOWLEDGMENTS

This work has been funded by "Sapienza - University" Grant 2015 no. C26H15Y42B (S.M.); by Istituto Pasteur Italia-Fondazione Cenci Bolognetti Project n. AT-24.2 (S.M); Grant 17\_RDB\_RUGHETTI\_Sap\_ProgMedi\_2016 (A.R.) and Ateneo 2016 (C.N). We are most grateful to Dr. Marialetizia Palomba and Mr. Marco Cristiani for helpful collaboration throughout this work. We specially thank Dr. Federica Capolunghi for critical reading of the manuscript and Dr. Ilary Ruscito for performing statistical analysis.

#### DISCLOSURES

None

## REFERENCES

1. Mattiucci S, Nascetti G. Advances and trends in the molecular systematics of anisakid nematodes, with implications for their evolutionary ecology and host-parasite co-evolutionary processes. *Adv. Parasitol.* 2008;66:47-148.
2. Mattiucci S, Cipriani P, Levsen A, Paoletti M, Nascetti G (2018). Molecular epidemiology of *Anisakis* and Anisakiasis: An Ecological and Evolutionary Road Map. *Adv Parasitol* 99, in press. doi.org/10.1016/bs.apar.2017.12.001
3. Mattiucci S, Cipriani P, Webb SC, et al. Genetic and morphological approaches distinguish the three sibling species of the *Anisakis simplex* species complex, with a species designation as *Anisakis berlandi* n. sp. for *A. simplex* sp. C (Nematoda: Anisakidae). *J. Parasitol.* 2014;100:199-214.
4. D'Amelio S, Mathiopoulos KD, Brandonisio O, Lucarelli G, Doronzo F, Paggi L. Diagnosis of a case of gastric anisakidosis by PCR-based restriction fragment length polymorphism analysis. *Parassitologia.* 1999;41:591-593.
5. Umehara A, Kawakami Y, Araki J, Uchida A. Molecular identification of the etiological agent of the human anisakiasis in Japan. *Parasitol. Int.* 2007;56:211-215.
6. Mattiucci S, Paoletti M, Borrini F, et al. First molecular identification of the zoonotic parasite *Anisakis pegreffii* (Nematoda: Anisakidae) in a paraffin-embedded granuloma taken from a case of human intestinal anisakiasis in Italy. *BMC Infect. Dis.* 2011;31:82.

- Accepted Article
7. Mattiucci S, Fazii P, De Rosa A, et al. Anisakiasis and gastroallergic reactions associated with *Anisakis pegreffii* infection, Italy. *Emerg. Infect. Dis.* 2013;19:496-499.
  8. Lim H, Jung BK, Cho J, Yooyen T, Shin EH, Chai JY. Molecular diagnosis of cause of anisakiasis in humans, South Korea. *Emerg. Infect. Dis.* 2015;21:342-344.
  9. Mladineo I, Popović M, Drmić-Hofman I, Poljak V. A case report of *Anisakis pegreffii* (Nematoda, Anisakidae) identified from archival paraffin sections of a Croatian patient. *BMC Infect. Dis.* 2016;16:42.
  10. Mattiucci S, Colantoni A, Crisafi B, et al. IgE sensitization to *Anisakis pegreffii* in Italy: comparison of two methods for the diagnosis of allergic anisakiasis. *Parasit. Immunol.* 2017a;39(7).
  11. Mattiucci S, Cipriani P, Paoletti M, Levsen A, Nascetti G. Reviewing biodiversity and epidemiological aspects of anisakid nematodes from the North East Atlantic Ocean. *J. Helminth.* 2017b. doi:10.1017/S0022149X1700027X.
  12. Nieuwenhuizen NE. *Anisakis* - immunology of a foodborne parasitosis. *Parasite Immunol.* 2016, 38:548-557.

13. Daschner A, Cuéllar C, Rodero M. The *Anisakis* allergy debate: does an evolutionary approach help? *Trends Parasitol.* 2012;28:9-15.
14. Alonso-Gómez A, Moreno-Ancillo A, López-Serrano MC, et al. *Anisakis simplex* only provokes allergic symptoms when the worm parasitises the gastrointestinal tract. *Parasitol. Res.* 2004;93:378-384.
15. Baeza ML, Conejero L, Higaki Y, et al. *Anisakis simplex* allergy: a murine model of anaphylaxis induced by parasitic proteins displays a mixed Th1/Th2 pattern. *Clin. Exp. Immunol.* 2005;142: 433–440.
16. Entwistle LJ, Wilson MS. MicroRNA-mediated regulation of immune responses to intestinal helminth infections. *Parasit Immunol.* 2017;39. doi: 10.1111/pim.12406.
17. Cortés A, Muñoz-Antoli C, Esteban JG, Toledo R. Th2 and Th1 Responses: Clear and Hidden Sides of Immunity Against Intestinal Helminths. *Trends Parasitol.* 2017. doi:10.1016/j.pt.2017.05.004. [Epub ahead of print]
18. Ueno H, Klechevsky E, Morita R, et al. Dendritic cell subsets in health and disease. *Immunol. Rev.* 2007;219:118-142.

19. Pulendran B. The varieties of immunological experience: of pathogens, stress, and dendritic cells. *Ann Rev Immunol.* 2015; 33:563-606.
20. Motran CC, Ambrosio LF, Volpini X, Celas DP, Cervi L. Dendritic cells and parasites: from recognition and activation to immune response instruction. *Semin Immunopathol.* 2017;39:199-213.
21. Klaver EJ, Kuijk LM, Laan LC, et al. *Trichuris suis*-induced modulation of human dendritic cell function is glycan-mediated. *Int. J. Parasitol.* 2013;43:191-200.
22. Hiemstra IH, Klaver EJ, Vrijland K, et al. Excreted/secreted *Trichuris suis* products reduce barrier function and suppress inflammatory cytokine production of intestinal epithelial cells. *Mol. Immunol.* 2014;60:1-7.
23. Mattiucci S, Acerra V, Paoletti M, et al. No more time to stay 'single' in the detection of *Anisakis pegreffii*, *A. simplex* (*s. s.*) and hybridization events between them: a multi-marker nuclear genotyping approach. *Parasitology.* 2016;143:998-1011.
24. Rughetti A, Rahimi H, Belleudi F, et al. Microvesicle cargo of tumor-associated MUC1 to dendritic cells allows cross-presentation and specific carbohydrate processing. *Cancer Immunol Res.* 2014;2:177-186.
25. Battisti F, Napoletano C, Rahimi Koshkaki H, et al. Tumor-derived microvesicles modulate antigen cross-processing via reactive oxygen species-mediated



alkalinisation of phagosomal compartment in Dendritic Cells. *Front. Immunol.* 2017; 8:1179.

26. Kotsias F, Hoffmann E, Amigorena S, Savina A. Reactive oxygen species production in the phagosome: impact on antigen presentation in dendritic cells. *Antioxid. Redox Signal.* 2013;18,:714-729.

27. Blanco P, Palucka AK, Pascual V, Banchereau J. Dendritic cells and cytokines in human inflammatory and autoimmune diseases. *Cytokine Growth Factor Rev.* 2008; 19:41-52.

28. Rescigno M. Dendritic cell functions: Learning from microbial evasion strategies. *Semin. Immunol.* 2015;27:119-124.

29. Coakley G, Maizels RM, Buck AH. Exosomes and Other Extracellular Vesicles: The New Communicators in Parasite Infections. *Trends Parasitol.* 2015;31:477-489.

30. Hartmann W, Brenz Y, Kingsley MT, et al. Nematode-derived proteins suppress proliferation and cytokine production of antigen-specific T cells via induction of cell death. *PLoS One.* 2013; 21, e68380.

31. Das Mohapatra A, Panda SK, Pradhan AK, Prusty BK, Satapathy AK, Ravindran B. Filarial antigens mediate apoptosis of human monocytes through Toll-like receptor 4. *J. Infect. Dis.* 2014; 210:1133-1144.

- Accepted Article
32. Babal P, Milcheva R, Petkova S, Janega P, Hurnikova Z. Apoptosis as the adaptation mechanism in survival of *Trichinella spiralis* in the host. *Parasitol. Res.* 2011;109:997-1002.
  33. Giri BR, Roy B. *Cysticercus fasciolaris* infection induced oxidative stress and apoptosis in rat liver: a strategy for host-parasite cross talk. *Parasitol. Res.* 2016;115:2617-2624.
  34. Messina CM, Pizzo F, Santulli A, et al. *Anisakis pegreffii* (Nematoda: Anisakidae) products modulate oxidative stress and apoptosis-related biomarkers in human cell lines. *Parasit. Vectors.* 2016;9:607.
  35. Johnson LA, Jackson DG. Control of dendritic cell trafficking in lymphatics by chemokines. *Angiogenesis.* 2014;17:335-345.
  36. Kuijk LM, Klaver EJ, Kooij G, et al. Soluble helminth products suppress clinical signs in murine experimental autoimmune encephalomyelitis and differentially modulate human dendritic cell activation. *Mol. Immunol.* 2012;51:210-218.
  37. Gruden-Movsesijan A, Ilic N, Colic M, et al. The impact of *Trichinella spiralis* excretory-secretory products on dendritic cells. *Comp. Immunol. Microbiol. Infect. Dis.* 2011;34:429-439.

38. Aranzamendi C, Fransen F, Langelaar M, et al. *Trichinella spiralis*-secreted products modulate DC functionality and expand regulatory T cells *in vitro*. *Parasite Immunol.* 2012;34:210-223.
39. Silva SR, Jacysyn JF, Macedo MS, Faquim-Mauro EL. Immunosuppressive components of *Ascaris suum* down-regulate expression of costimulatory molecules and function of antigen-presenting cells via an IL-10-mediated mechanism. *Eur. J. Immunol.* 2006;36:3227-3237.
40. Dowling DJ, Noone CM, Adams PN, et al. *Ascaris lumbricoides* pseudocoelomic body fluid induces a partially activated dendritic cell phenotype with Th2 promoting ability *in vivo*. *Int. J. Parasitol.* 2011;41:255-261.
41. Nakahara T, Moroi Y, Uchi H, Furue M. Differential role of MAPK signaling in human dendritic cell maturation and Th1/Th2 engagement. *J Dermatol Sci.* 2006;42:1-11.
42. Terrazas CA, Huitron E, Vazquez A, et al. MIF synergizes with *Trypanosoma cruzi* antigens to promote efficient dendritic cell maturation and IL-12 production via p38 MAPK. *Int. J. Biol. Sci.* 2011;7:1298-1310.
43. Cvetkovic J, Sofronic-Milosavljevic L, Ilic N, Gnjatovic M, Nagano I, Gruden-Movsesijan A. Immunomodulatory potential of particular *Trichinella spiralis* muscle larvae excretory-secretory components. *Int. J. Parasitol.* 2016;46:833-842.

44. Annunziato F, Romagnani S. Heterogeneity of human effector CD4<sup>+</sup> T cells. *Arthritis Res. Ther.* 2009;11:257.
45. Allen JE, Maizels RM. Diversity and dialogue in immunity to helminths. *Nat. Rev. Immunol.* 2011;11:375-388.
46. Gerbe F, Sidot E, Smyth DJ, et al. Intestinal epithelial tuft cells initiate type 2 mucosal immunity to helminth parasites. *Nature.* 2016;529:226-230.
47. Lian J, Luster AD. Chemokine-guided cell positioning in the lymph node orchestrates the generation of adaptive immune responses. *Curr. Opin. Cell. Biol.* 2015;36:1-6.
48. Witkowska AM, Borawska MH. Soluble intercellular adhesion molecule-1 (sICAM-1): an overview. *Eur. Cytokine Netw.* 2004;15:91-98.
49. Morris MA, Ley K. Trafficking of natural killer cells. *Curr. Mol. Med.* 2004;4:431-438.
50. Becher B, Tugues S, Greter M. GM-CSF: From Growth Factor to Central Mediator of Tissue Inflammation. *Immunity.* 2016;45:963-973.
51. Ivanova EA, Orekhov AN. T Helper Lymphocyte Subsets and Plasticity in Autoimmunity and Cancer: An Overview. *Biomed. Res. Int.* 2015; 327470:9.

52. Zizzari IG, Napoletano C, Battisti F, et al. MGL receptor and immunity: when the ligand can make the difference. *J. Immunol. Res.* 2015;450695.
53. Iborra S, Martínez-López M, Cueto FJ, et al. *Leishmania* Uses Mincle to Target an Inhibitory ITAM Signaling Pathway in Dendritic Cells that Dampens Adaptive Immunity to Infection. *Immunity.* 2016;45:788-801.
54. Rodríguez E, Anadón AM. Novel sequences and epitopes of diagnostic value derived from the *Anisakis simplex* Ani s 7 major allergen. *Allergy.* 2008;63:219-225.
55. Swofford DL. PAUP\*. Phylogenetic analysis using parsimony (\*and other Methods). Sunderland, MA. *Sinauer Associates* 2003.
56. Hall TA. BioEdit: a user-friendly biological sequence alignment editor and analysis program for Windows 95/98/NT. *Nucl. Acids Symp. Ser.* 1999;41:95-98.

#### LEGENDS TO THE FIGURES

**FIGURE 1.** Maximum Parsimony (MP) consensus tree based on mtDNA *cox2* gene sequences of *A. pegreffii* larvae from *E. encrasicolus* and *Merluccius merluccius* from Adriatic Sea, (used for incubation with DCs and CE preparation) with respect to the other *Anisakis* spp. That were previously sequenced. The analysis was performed by PAUP4\*,<sup>55</sup> using Bootstrap values (>70) reported at the nodes; *Toxocara canis* and *Ascaris suum* were used as outgroups.

**FIGURE 2.** Alignment, by using BioEdit,<sup>56</sup> of the EF1  $\alpha$ -1 nDNA (409 bp) sequences of *A. pegreffii* larvae, (used for incubation with DCs and CE preparation), with respect to those of *A. pegreffii* and *A. simplex* (s. s) previously sequenced and deposited in GenBank.<sup>23</sup> The relative electropherograms of these genotypes are also reported below. The arrows are showing the fixed nucleotide diagnostic positions (as indicated in the text) between *A. pegreffii* and *A. simplex* (s.s.). Dots indicate identity; standard IUPAC codes were used. Accession numbers of sequences of *A. pegreffii* at the EF1  $\alpha$ -1 nDNA gene, deposited in GenBank, are reported in the text.

**FIGURE 3.** Live larvae (L) of *A. pegreffii* induce apoptosis, alter DC phenotype and activates ERK1,2 and NF $\kappa$ B pathways. A. Histograms represent the percentage of live cells obtained after 6 days of DC culture. DCs were differentiated and matured in absence of the larvae (iDCs and mDCs) and in presence of the live parasite (iDCs+L and mDCs+L). Data are reported as mean percentage of live cells derived from 4 donors  $\pm$  standard deviation B. Expression of HLA-DR, CD86, CD83 and CCR7 markers obtained by flow cytometry from 4 donors in differently treated DCs. Data are reported as values of Mean Fluorescence Intensity (MFI) C. Western blotting of differently treated DC lysates. Cell lysates were stained with pERK1,2 and p50/105.  $\alpha$ -tubulin was used as loading control. Samples were run in 4-15% SDS-PAGE gels and were analysed in reducing conditions. These results are representative of one donor out of three.

**FIGURE 4.** CE of *A. pegreffii* activates DC apoptosis, modulates DC phenotype and triggers ERK1,2 and NF $\kappa$ B pathways. A. Histograms represent the percentage of live cells obtained after 6 days of DC culture. DCs were differentiated and matured in absence (iDCs and mDCs) and in the presence of the OM (iDCs and mDCs). Data are reported as mean percentage of live cells derived from 9 donors  $\pm$  standard deviation B. Expression of HLA-DR, CD86, CD83 and CCR7 markers obtained by

cytofluorimetry from 9 donors in iDCs and mDCs alone or in presence of the OM. Data are reported as values of Mean Fluorescence Intensity (MFI). C. Western blotting of differently treated DC lysates.

Cell lysates were stained with pERK1,2 and p50/105.  $\alpha$ -tubulin was used as loading control. Samples were run in 4-15% SDS-PAGE gels and were analysed in reducing conditions. These results are representative of one donor out of four.

**FIGURE 5.** ROS measurement at 30 minutes of chase. iDCs or mDCs+CE (grey histograms) and iDCs or mDCs+L (black histograms) have a significant higher ROS molecules compared to iDCs or mDCs (white histograms). ROS levels are plotted as arbitrary units of three independent experiments. ROS level in iDCs at time 30 of chase corresponded to 100 arbitrary units. Significance was evaluated as Student *t* test pairing DC control sample vs DCs+L experimental sample or DC+CE experimental sample. Anova test was employed to evaluate significative differences among the iDCs or the mDCs samples, while *t* Student test for paired samples. \**p*<0.05, \*\**p*<0.01, \*\*\**p*<0.001.

**FIGURE 6.** Live larvae (L) and CE of *A. pegreffii* modulate the cytokines and chemokines released by DCs (three donors). The amount of sICAM, CXCL10, CCL4, CCL3, IL6, IL1 $\alpha$ , IL4, IL10 and GM-CSF were measured in differently treated DC culture supernatants by Luminex multiplex beads analysis after 48 hours of PMA/Ionomycin stimulation. Secretion range for each molecule was as follow: sICAM: 7,7-12,4  $\mu$ g/mL (iDCs)/12-16  $\mu$ g/mL (mDCs); CXCL10: 25-130 ng/mL (iDCs)/57-138 ng/mL (mDCs); CCL3: 0,376-1,4  $\mu$ g/mL (iDCs)/0,448-1,7  $\mu$ g/mL (mDCs); CCL4: 19-84  $\mu$ g/mL (iDCs)/22-96  $\mu$ g/mL (mDCs); IL6: 116-273 ng/mL (iDCs)/0,3-3  $\mu$ g/mL (mDCs); IL1 $\alpha$ : 36-56 ng/mL (iDCs)/46-98 ng/mL (mDCs); IL10: 10-39 ng/mL (iDCs)/25-42 ng/mL (mDCs); IL4: 0,107-6,3  $\mu$ g/mL (iDCs)/0,15-8,4  $\mu$ g/mL (mDCs). For each experiment, Values obtained for iDCs and mDCs control samples were set as 100% and the corresponding cytokine/chemokine measurement for the experimental DC group

compared and calculated as percentage.

Significance was evaluated as Student *t* test pairing DCs control samples vs DCs+L experimental group or DCs control samples vs DCs+CE experimental group. \*  $p < 0.05$ , \*\*  $p < 0.01$ , \*\*\*  $p < 0.001$ .

**FIGURE 7.** DCs treated with the live parasite (L) and the CE of *A. pegreffii* reduces the production of IFN $\gamma$  by T cells. Differently treated DCs were co-cultured for 4 days with naïve T lymphocytes. T cells were then stimulated for 16-18 hours with PMA/Ionomycin in presence of Brefeldin. The production of IFN $\gamma$ , IL4, IL10 and IL17 were analysed as intracellular staining. Data are reported as mean percentage of cytokine-producing cells derived from 4 donors  $\pm$  standard deviation. Significance was evaluated as Anova test among the three experimental conditions for each set of iDC or mDCs.

Student *t* test pairing DCs control samples vs DCs+L experimental samples or DCs control samples vs DC+CE experimental samples. \*  $p < 0.05$ , \*\*  $p < 0.01$ , \*\*\*  $p < 0.001$ .

Anova test indicated significance only for the IFN $\gamma$  production induced by iDCs ( $p < 0,05$ ); in particular iDC+CE were significantly poor stimulator for IFN $\gamma$  production as compared to iDCs ( $p < 0,05$ ).

#### LEGENDS TO SUPPLEMENTARY FIGURES

**SUPPLEMENTARY FIGURE 1.** Phagosomal ROS analysis of DCs by flow cytometry: gating strategy and analysis of DC samples. DCs were pulsed with DHR132 (FL1)/FP467(FL4) coupled beads (3  $\mu$ m). After washing, DCs were analysed by flow cytometry to evaluate phagosomal ROS. The gating and analysis of iDCs (first row, panels a-c), iDCs+CE (second row, panels d-f) and iDCs+L (third row, panels g-i) are depicted. DCs were identified and gated by physical parameters SSC-A/FSC-A (panels a, d, g) Subsequently, the gated cells were plotted by SSC-A and SSC-W, parameters that allow distinguishing single cells from double or multiple cells; the single DCs were then gated (dot plot b, e,



h). The gated single cell DCs population was then plotted by fluorescence parameters (APC-A/FL4, *y axis*; FITC-A/DHR132 (*x axis*) (dot plot c, f, i). The double positive events corresponded to DCs that have phagocytated one, two or more beads. A third gating was made to select the double positive cells that had phagocytated one bead/cell. The mean Fluorescence Intensity of FL1 and FL4 was calculated for this latter gated cell population. The ratio between FL1 (ROS sensitive) and FL4(ROS insensitive) of iDCs was set as 100% ROS arbitrary Units. The FL1/FL4 ratio of DC experimental samples is then related to the FL1/FL4 ratio of DC control sample and converted in percentage (see Supplementary Table 1).

**SUPPLEMENTARY FIGURE 2.** Flow cytometry analysis of the T cell mediated IFN $\gamma$  production in one representative donor. Panel A) gating of T cells (first column) and analysis of the T cell mediated IFN $\gamma$  production (second column) after stimulation with iDC (first row), iDCs+L (second row), iDCs+CE (third row). T cells were plotted for the physical parameter SSC-A (*y axis*) and FSC (*x axis*) (first column). The gate P1 identified the cells that were analysed by IFN $\gamma$  production (second column) [IFN $\gamma$ -FITC/FL1(*y axis*) and FSC (*x axis*)]. The events above the gate for FITC control were then considered positive and percentage calculated and reported in the plot. Panel B similarly depicts T cell gating and T cell mediated IFN $\gamma$  production of T cells stimulated with mDCs (first row), mDCs+L (second row) and mDCs+CE /third row).

**SUPPLEMENTARY FIGURE 3.** Phenotype characterization and viability of DCs exposed to live larvae of one representative donor. A) Gating of DCs population by flow cytometry physical parameters [SSC-A (*y axis*) and FSC (*x axis*)]; B) Apoptosis analysis by double staining PI(FL4)/Annexin V (FL1) of iDCs, iDCs+L, mDCs, mDCs+L, respectively. The percentage of cells undergoing apoptosis corresponded to the sum of double positive cells and Annexin V-positive cells. C) Phenotype analysis of iDCs, (first column), iDCs+L (second column), mDCs (third column), mDCs+L (fourth column).

Fluorescence signal associated to the cells is plotted as histograms. Mean Fluorescence Intensity (MFI) of each histogram is reported. In first row and in fifth row the FITC-isotype and PE-isotype, respectively are reported.

**SUPPLEMENTARY FIGURE 4.** Phenotype characterization and viability of DCs exposed to CE of one representative donor. A) Gating of DCs population by flow cytometry physical parameters [SSC-A (*y axis*) and FSC (*x axis*)]; B) Apoptosis analysis by double staining PI(FL4)/Annexin V (FL1) of iDCs, iDCs+CE, mDCs, mDCs+CE. The percentage of cells undergoing apoptosis corresponded to the sum of double positive cells and Annexin V-positive cells. C) Phenotype analysis of iDCs, (first column), iDCs+CE (second column), mDCs (third column), mDCs+CE/fourth column). Fluorescence signal associated to the cells is plotted as histograms. Mean Fluorescence Intensity (MFI) of each histogram is reported. In first row and in fifth row the FITC-isotype and PE-isotype respectively are reported.



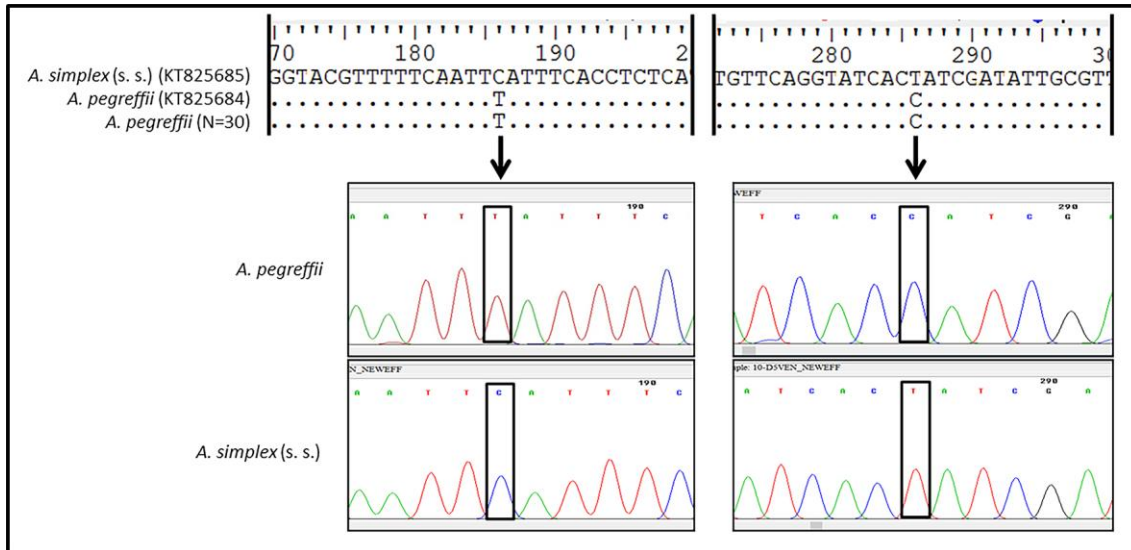


**Figure 3**

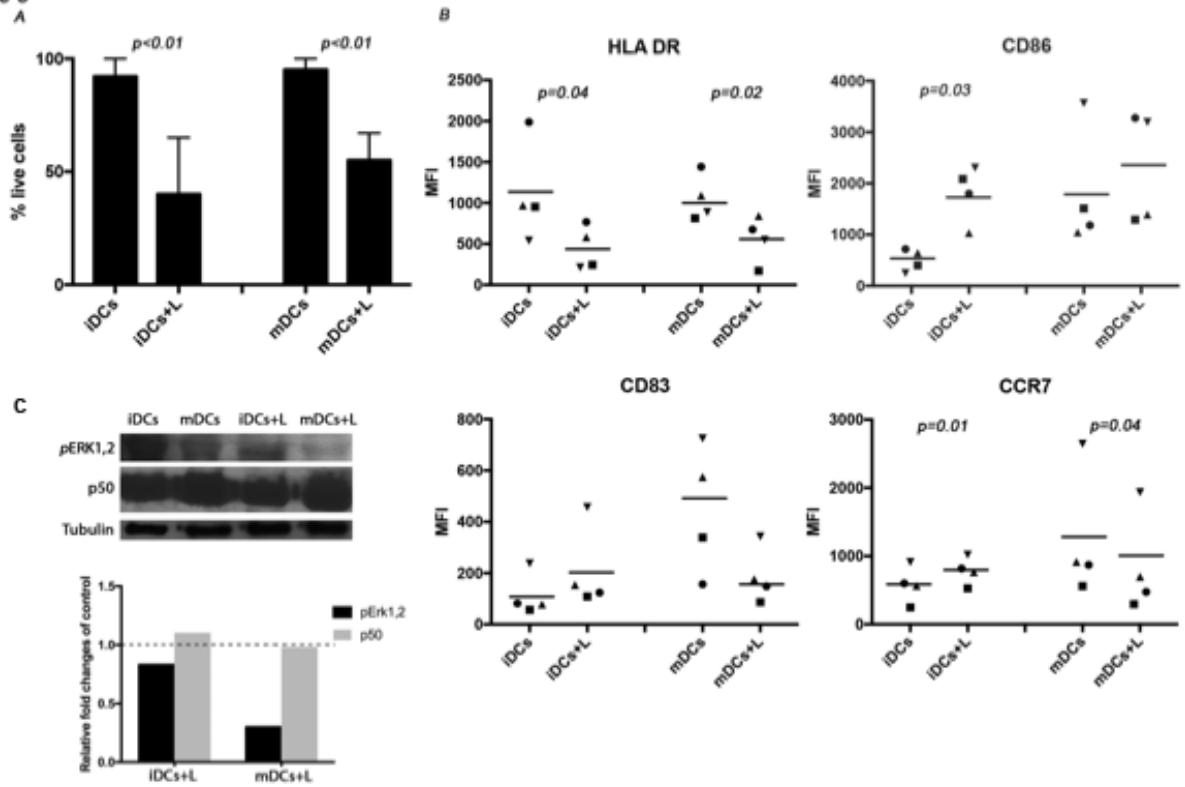


Figure 4

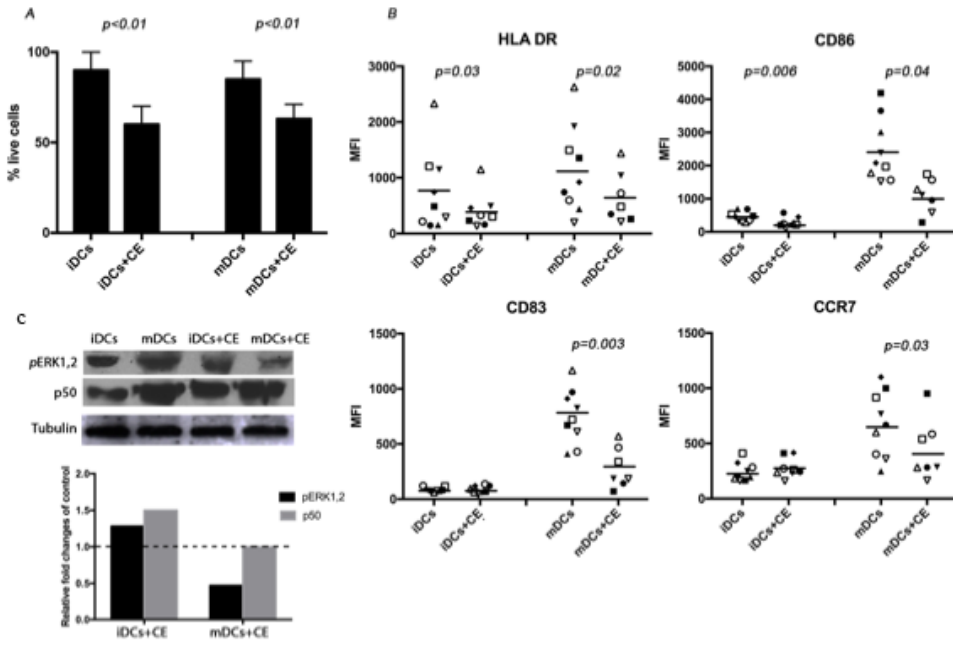


Figure 5

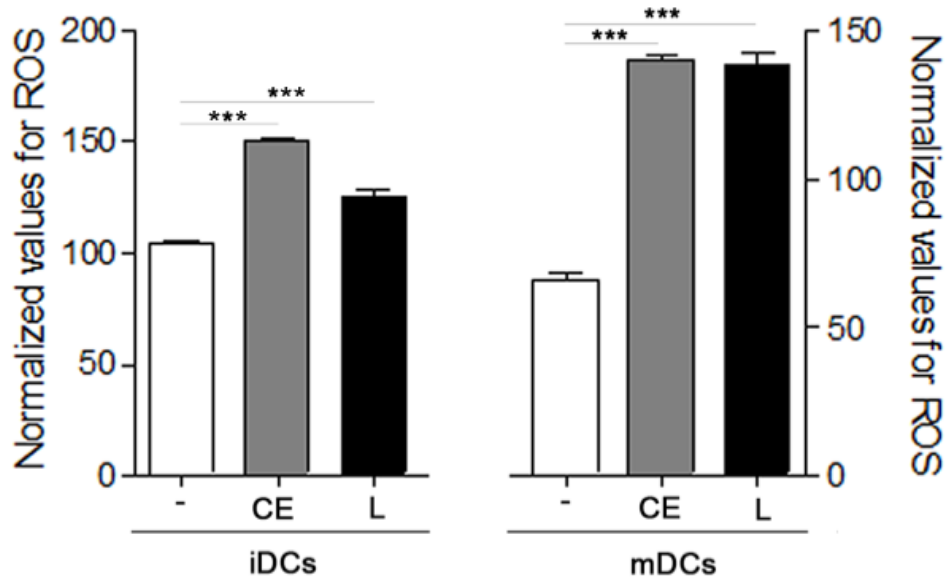


Figure 6

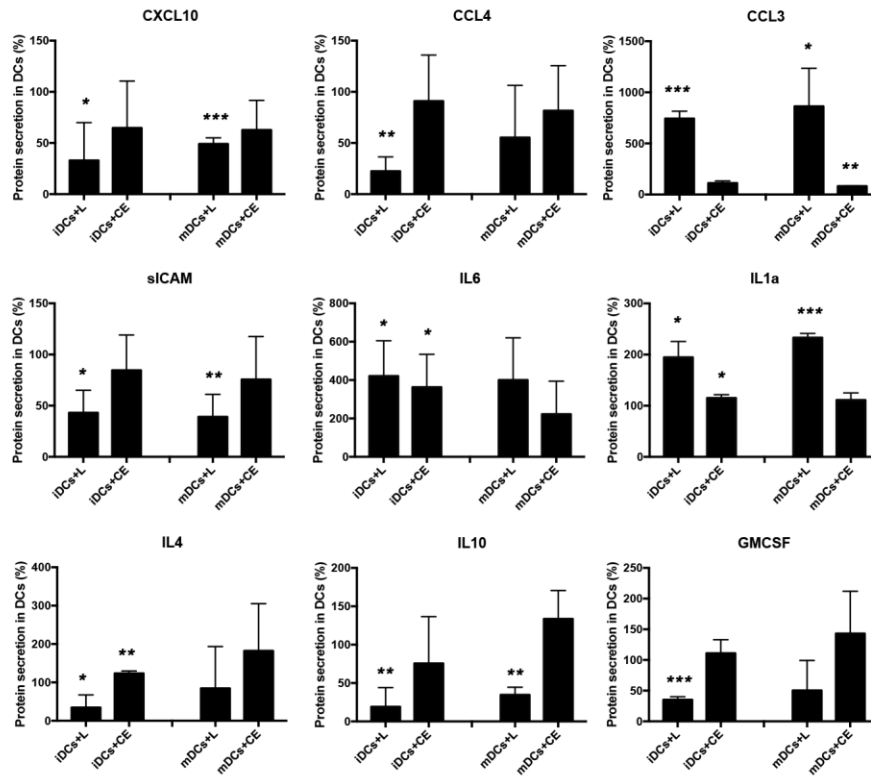


Figure 7

